ELSEVIER

Catalysis Today 68 (2001) 209–216

CATALYSIS TODAY

www.elsevier.com/locate/cattod

High activity in catalytic cracking over stable mesoporous aluminosilicates

Lei Zhu, Feng-Shou Xiao*, Zongtao Zhang,
Yinyong Sun, Yu Han, Shilun Qiu

*Department of Chemistry and Key Laboratory of Inorganic Synthesis and Preparative Chemistry,
Jilin University, Changchun 130023, PR China*

Abstract

A stable mesoporous aluminosilicate with hexagonal symmetry (MAS-5) has been synthesized by the co-templates of tetraethylammonium hydroxide (TEAOH) and cetyltrimethylammonium bromide (CTAB) cationic surfactant. The cracking of 1,3,5-triisopropylbenzene is used as probe reaction to test its catalytic properties. Catalytic data show that the conversion over the stable mesoporous aluminosilicate (HMAS-5) is higher than that over HA1-MCM-41, which is assigned to HMAS-5 which has stronger acidity than HAl-MCM-41. Furthermore, we observed that the catalytic conversion over HMAS-5 is much higher than that over HZSM-5, which is assigned to that the diffusion of large molecule of 1,3,5-triisopropylbenzene is strongly impeded by narrow channels of HZSM-5 zeolite.

Keywords: Mesoporous; MCM-41; ZSM-5; Hydrothermal stability; Catalytic cracking

1. Introduction

Molecular sieves with large pore size are much in demand for reactions involving large molecules such as residue cracking [1,2]. Since the development of MCM-41 by Mobil scientists in 1992 [3,4], many attempts have been made not only to improve its structural stability, but also to increase its catalytic activity and selectivity.

Being the most important member of the mesostructured materials, MCM-41 with its hexagonal array of pores was conceived to carry out catalytic cracking process of bulky molecules [5,6]. The advantage of mesoporous materials for acid-catalytic reactions are based on the presence of large regular pores which allow the diffusion of reactants and conversely the fast diffusion of the products out, minimizing unwanted consecutive reactions and catalyst decay. Unfortunately, MCM-41 shows very weak acidity as compared with that of microporous zeolites such as HZSM-5 [7].

Additionally, these mesoporous materials show low hydrothermal stability. Therefore, the mesoporous materials with better hydrothermal stability are always considered [8,9].

HZSM-5 has strong acidity and perfect selectivity in many catalytic reactions, and it is widely used in acid-catalyzed reactions for the production of fuels, petrochemicals, and fine chemicals [10–12]. ZSM-5 has two-dimensional tunnels parallel to either axis *a* or axis *c*. Its pores have 10-ring apertures with dimensions of 5.4 Å × 5.6 Å or 5.1 Å × 5.5 Å, respectively. These structural characters suggest that the inner catalytic sites are accessible to small molecular

---

* Corresponding author. Tel.: +86-431-892-2331;
fax: +86-431-567-1974.
E-mail address: fsxiao@mail.jlu.edu.cn (F.-S. Xiao).

0920-5861/01/$ – see front matter
PII: S0920-5861(01)00302-9

but inaccessible to such bulk molecule as 1,3,5-triisopropylbenzene.

The goal of this work is to find mesoporous aluminosilicates with high catalytic activity in cracking of 1,3,5-triisopropylbenzene as a model reaction for catalytic cracking of large molecules [13].

2. Experimental

2.1. Materials

Isopropylbenzene (AR), tetraethylammonium hydroxide (TEAOH), and cetyltrimethylammonium bromide (CTAB) were supported by Beijing Chemical, and triisopropylbenzene (CP) was purchased from Aldrich Chemical.

The molecular sieves such as ZSM-5 and MCM-41 were synthesized according to published literatures [3,14]. Mesoporous aluminosilicate denoted as MAS-5 was hydrothermally synthesized from starting materials of silica and sodium aluminate in the presence of co-templates of TEAOH and CTAB cationic surfactant with molar ratio of $Al_2O_3/SiO_2/TEAOH/CTAB/H_2O$ at 1.0–6.5/28.0–350/10.0–63.0/12.0–32.0/500–2000, respectively. First, sodium aluminate was mixed with TEAOH solution, followed by addition of silica. After treatment of the mixture for several hours, the starting precursors were formed, which was further added into the CTAB. Then, the mixture was crystallized at 50–150°C for several days. As a typical run, (1) 0.236–1.360 g of sodium aluminate, 0.110–0.400 g of sodium hydroxide, and 26.000–36.000 g of TEAOH (20 wt.% aqueous solution) were mixed in a plastic vessel. Then 10.086 g of fume silica was added, stirring for several hours. After becoming homogeneous solution, the resulting mixture was transferred to Teflon-lined stainless-steel autoclaves and heated to 100–150°C for several hours, forming aluminosilicate precursors, (2) 1.180–1.920 g of CTAB and 25.000 g of deionized water were mixed, which was added into 9.8 g of aluminosilicate precursors. Then, the resulting mixture was transferred to Teflon-lined stainless-steel autoclaves again, heating at 100–150°C in oven [15]. All the molecular sieve samples were characterized by powder X-ray diffraction (XRD) before catalytical test. The molar ratio of Si/Al in MAS-5 products could be varied at 12–700.

2.2. Methods of characterization

The powder XRD data were collected on a Siemens D5005 Diffractometer using Cu $K\alpha$ radiation at 40 kV and 30 mA, with the scanning rate of 4°/min (2θ). The sample isotherms of nitrogen at the temperature of liquid nitrogen were measured using a Micromeritics ASAP 2010 system. The samples were outgassed for 2 h at 400°C before the measurements. The pore size distributions for micropores and mesopores were calculated using Horvath–Kawazoe (HK) model and Barrett–Joyner–Halenda (BJH) model, respectively. Si/Al ratios of the samples was measured by Perkin-Elmer 3300 DV ICP, NMR, and chemical analysis.

An FT-IR spectroscopy, Impact 410, Nicolet, was used in the pyridine adsorption method. Before measurement of pyridine adsorption, the samples were pressed to thin wafers (5 mg/cm^2), and were placed into quartz cell equipped with CaF_2 windows. The sample disks were evacuated at 400°C for 2 h (10^{-5} Torr) and cooled down to room temperature, then 10 Torr of pyridine was exposed to the disks at room temperature. After the adsorption at room temperature for 1 h and evacuation at 150°C for 1 h, the infrared spectra were recorded.

2.3. Catalytic reactions of isopropylbenzene and 1,3,5-triisopropylbenzene

Samples were calcinated at 600°C for 5 h to burn off remaining organic template. Pretreatment of the catalysts was performed by ion-exchanges in NH_4Cl (1 N, 100 ml solution for 1 g sample) at 80°C for 4 h and a subsequent calcination at 773 K to make the activated proton samples. The catalytic testing was performed by pulse method, and analyses of the cracking products were carried out using a GC-8A equipped with a TCD detector. As a typical run, 0.051 g of catalyst mass and 0.4 μl of 1,3,5-triisopropylbenzene or isopropylbenzene were used at carrier gas of nitrogen with the flowing rate of 55 ml/min. The reaction temperatures are in the range of 250–320°C (no thermal cracking).

Blank experiments were also carried out under the same reaction conditions but without catalyst in the reactor. None of the cracking products were observed in these blank experiments, even at the highest temperature used in this work.

3. Results and discussion

3.1. Hydrothermal stability of MAS-5 and MCM-41

Hydrothermal stability of mesostructured materials has been widely investigated, and several successful examples have been reported. Ryoo et al. synthesized mesoporous KIT-1, exhibiting higher hydrothermal stability than MCM-41; Zhao et al. [8] reported hexagonal mesoporous SBA-15, which is stable in boiling water for over 48 h; Pinnavaia and co-workers [9] reported mesostructured MSU-G, keeping its structure in boiling water for over 150 h.

Fig. 1A shows XRD patterns of as-synthesized MAS-5, showing four well-resolved peaks in the region of 2–6°, which are indexable as (1 0 0), (1 1 0), (2 0 0), (2 1 0) reflections associated with hexagonal symmetry. Interestingly, after treatment of the calcined sample in boiling water over 300 h (Fig. 1B), the XRD patterns also show similar peaks assigned to hexagonal mesopores, suggesting that the MAS-5 is very hydrothermally stable. Furthermore, even if the HMAS-5 is heated in water vapor at 800°C for 2 h, the characteristic peaks assigned to hexagonal mesopores still remained, which suggest that at high temperature HMAS-5 is hydrothermally (steaming) stable. In contrast, Al-MCM-41 loses its structure after the treatment of boiling water for 10 h, as shown in Fig. 1C and D.

Table 1
BET surface area and pore size distribution of MCM-41, ZSM-5 and MAS-5 samples

Samples	Si/Al	Pore size (Å)	BET surface (m^2/g)
MCM-41	60	30	950
ZSM-5	64	5.6	380
MAS-5	61	27	1038

BET surface area and pore size of MAS-5 and MCM-41 samples have been characterized by nitrogen isotherms at liquid nitrogen temperature, and the data are presented in Table 1. Notably, the surface area

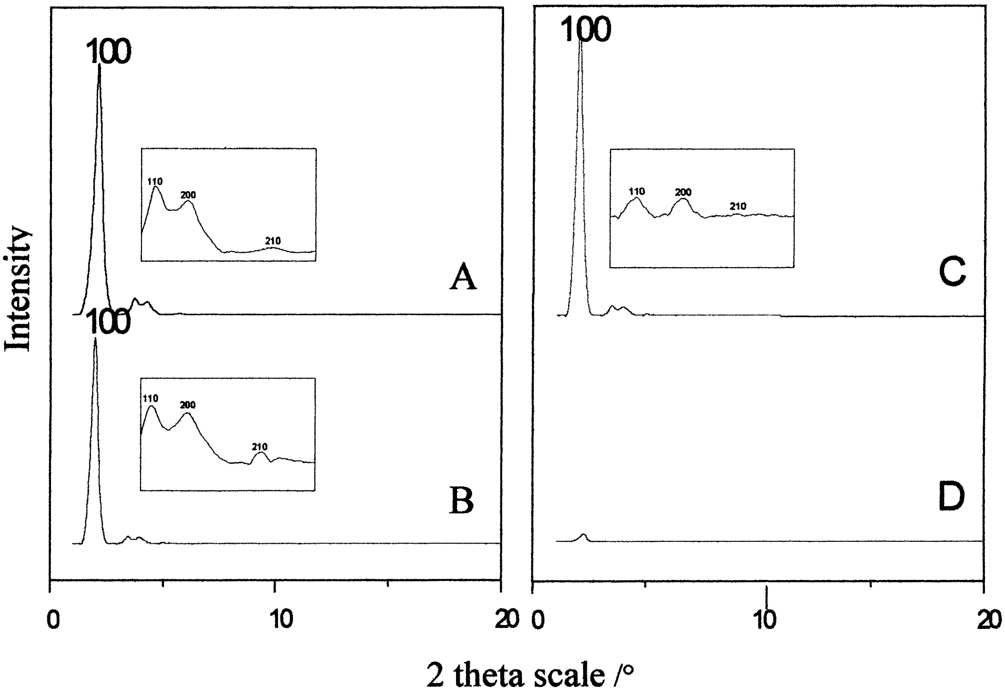

Fig. 1. XRD patterns of (A) as-synthesized MAS-5; (B) after calcination at 550°C to remove organic template, MAS-5 was treated in boiling water for 300 h; (C) as-synthesized MCM-41; (D) after calcination at 550°C to remove organic template MCM-41 was treated in boiling water for 24 h. Si/Al ratio of MAS-5 and MCM-41 is at 61 and 60, respectively.

Table 2
Catalytic activities in the cracking of isopropylbenzene over various samples of HMCM-41, HZSM-5, and HMAS-5 (a: product undetectable; b: product detectable but its content is below the record threshold)

Samples	Si/Al ratio	Conversion (mol%)	Selectivity			Temperature (°C)
			Benzene	*m*-Diisopropylbenzene	*p*-Diisopropylbenzene	
HMCM-41	60	5.4	100	a	a	250
		15.7	100	a	a	280
		21.9	93.7	6.3	b	300
		26.8	91.6	8.0	b	320
HZSM-5	64	79.3	100	a	a	250
		82.8	100	a	a	280
		83.5	100	a	a	300
		86.8	100	a	a	320
HMAS-5	61	8.6	100	a	a	250
		18.3	94.0	5.2	b	280
		25.8	87.5	7.9	4.5	300
		29.5	84.2	10.0	5.8	320

of MAS-5 (1038 m^2/g) is larger than that of MCM-41 (950 m^2/g), BJH pore size distribution of MAS-5 (27 Å) is very close to that of MCM-41 (30 Å).

3.2. Catalytic cracking of isopropylbenzene

As shown in Table 2, HZSM-5 exhibits the highest conversion in catalytic cracking of isopropylbenzene for the three samples. For example, HZSM-5 gives a conversion of 79.3% at 250°C, which is much higher than 5.4% of HMCM-41 and 8.6% of HMAS-5. Their results may be attributed to that HZSM-5 has much stronger acidity and specific selectivity than HMCM-41 and HMAS-5 in catalytic cracking of isopropylbenzene.

Furthermore, we observed that there are byproducts of diisopropylbenzene at the temperature of 300–320°C over catalysts of both HMCM-41 and HMAS-5, which could be resulted from catalytic alkylation of isopropylbenze with propylene formed by cracking of isopropylbenzene, due to the large pore size of mesoporous materials. Moreover, we find that HMAS-5 shows higher selectivity for diisopropylbenzene products than HMCM-41, which is assigned to stronger ability for the alkylation due to stronger acidic sites in HMAS-5. Additionally, we also observed that HMAS-5 shows higher conversion than HMCM-41, which is also assigned that HMAS-5 has stronger acidity than HMCM-41.

3.3. Catalytic cracking of 1,3,5-triisopropylbenzene over HZSM-5, HMCM-41, and HMAS-5 samples

Table 3 presents the catalytic data for 1,3,5-triisopropylbenzene over the samples of HZSM-5, HMCM-41, and HMAS-5. Obviously, HZSM-5 shows very low conversion, giving at 2.7% at 250°C, and the product is only *m*-diisopropylbenzene. The result suggests that HZSM-5 is basically inactive for catalytic cracking of large molecule of 1,3,5-triisopropylbenzene at low temperature, because ZSM-5 has 10-ring pores with diameter no larger than 5.6 Å, while 1,3,5-triisopropylbenzene has the dynamic diameter of 9.4 Å and cannot diffuse through the inner pores of ZSM-5. Possibly, the cracking of 1,3,5-triisopropylbenzene only occurs on the surface of HZSM-5 crystals, which has been confirmed by that smaller size of HZSM-5 crystals exhibit higher activity in the catalysis (Table 3).

In contrast, both HMAS-5 and HMCM-41 give high conversion. Additionally, HMAS-5 (79.8% at 250°C) is much higher than HMCM-41 (65.8% at 250°C), which is reasonably attributed that HMAS-5 has stronger acidity than HMCM-41.

Interestingly, although HMCM-41 shows high activity, it completely loses its activity after treatment in boiling water for 10 h. In contrast, HMAS-5 gives both higher activity and longer catalyst stability than HMCM-41. Even if HMAS-5 is treated in boiling water for 300 h, it still shows high catalytic activity,

Table 3
Catalytic activities in the cracking of triisopropylbenzene over various samples of HMCM-41, HZSM-5, and HMAS-5 (a: product undetectable; b: particle size of about 30 μ; c: particle size of about 5 μ)

Samples	Si/Al ratio	Conversion (mol%)	Selectivity				Temperature (°C)
			Benzene	Isopropylbenzene	*m*-Diisopropylbenzene	*p*-Diisopropylbenzene	
HMCM-41	60	65.8	a	28.4	51.0	20.6	250
		72.4	2.2	35.5	43.7	18.5	280
		80.1	6.4	41.0	38.6	13.7	310
HZSM-5	64	2.7	a	a	100	a	250
		8.0	a	18.2	74.0	7.7	280
		11.8b	a	17.7	66.3	14.9	310
		20.3c	a	20.5	58.9	18.6	310
HMAS-5	61	79.8	a	42.1	41.0	16.9	250
		85.1	7.3	46.3	33.1	13.2	280
		92.1	6.1	49.7	31.6	11.2	310

as shown in Table 4. These results also confirm that HMAS-5 has a high hydrothermal stability.

Furthermore, in the cracking of 1,3,5-triisopropylbenzene the product distribution over HMCM-41 and HMAS-5 is different. Over HMAS-5 the isopropylbenzene is major product, and over HMCM-41 the diisopropylbenzenes are major products. These results are reasonably resulted from the difference in acidic properties and cracking mechanisms. Possibly, HMAS-5 with stronger acidic strength has higher cracking ability than that of HMCM-41, giving higher selectivity for isopropylbenzene.

As investigated by Koch and Reschetilowski [16], under optimal conditions, Al-MCM-41 shows a high catalytic cracking activity for long-chain hydrocarbons such as 1,3,5-triisopropylbenzene, which is comparable with that of zeolite Y. Here our work shows that this HMSA-5 has an even higher catalytic activity than MCM-41, suggesting that HMSA-5 may be a helpful catalyst for catalytic cracking of residue.

3.4. Catalytic cracking of 1,3,5-triisopropylbenzene over various MAS-5 samples

Materials with different Na^+ content brings about different catalytic performances [17]. HMAS-5 and NaMAS-5 samples with the similar Si/Al ratio were prepared from ion-exchange method in NH_4Cl

Table 4
Catalytical cracking of 1,3,5-triisopropylbenzene over HMCM-41 and HMAS-5 samples treated by various methods (a: reaction temperature at 253°C; b: ion-exchange by NH_4Cl (aq. 1 N) to ammonium type of molecular sieve, followed by calcination to form protonated molecular sieve at 650°C; c: ion-exchange by NaCl (aq. 1 N) to sodium molecular sieves for 2 h to form sodium type of molecular sieve; d: product undetectable; e: calcinated MAS-5 without ion-exchange)

Sample	Si/Al	Treatment	Conversion (mol%)	
			Isopropylbenzene cracking	1,3,5-Triisopropylbenzene cracking
HMCM-41	60	b	5.4	66.1
		After a, the sample was heated in boiling water for 10 h	d	1.2
HMAS-5	61	b	8.6	82.7
		After a, the Sample was heated in boiling water for 300 h	8.9	80.4
	30	b	11.0	88.1
	15	b	12.5	91.8
NaMAS-5	61	c	0	11.6
MAS-5e	61	–	8.1	75.2

(aq. 1 N) and NaCl (aq. 1 N) and subsequent calcinations at 500°C. As presented in Table 4, the catalytic activity is improved after protonation, while NaMAS-5 shows very poor activity. These results indicate that acidic species are catalytically active sites in the catalytic cracking reactions.

HMAS-5 samples with different Si/Al ratios (calcinated at 550°C) are also compared, and we can see that the catalytic conversion decreases with the increase of Si/Al ratio. The results also suggest that the cracking activity is corresponding to the acidic sites, which resulted from framework Al species in the HMAS-5 catalyst.

3.5. Catalyst deactivation and regeneration in cracking of 1,3,5-triisopropylbenzene

The rapid loss of catalytic activity in cracking has a profound influence on the engineering and commercialization of cat cracking. In the cracking of small model molecules where there is no possibility of unknown poisons being responsible for the decay, it is well acknowledged that coke “laydown” is responsible for the consequent decay of activity [18]. It is clear that the loss of catalyst activity in catalytic cracking must be connected in some way with one or both of the following root causes: (1) the complete loss of some active sites; (2) various degrees of reduction in the activity (inhibition) of some or all sites.

In the cracking of 1,3,5-triisopropylbenzene, we noted that the process of decay has been amply demonstrated to be a function of the pulses of the feed of reactants. For example, in the beginning pulses of first five times, the catalytic conversion for triisopropylbenzene is at near 80–82%; when increasing pulses to 60, the catalytic conversion is reduced to 70%. As original activity can be fully restored by burning of the carbonaceous deposit formed during the cracking reaction, the sites themselves are not altered by the decay process in any permanent way. The most perfect regeneration was achieved at 700°C as shown in Fig. 2.

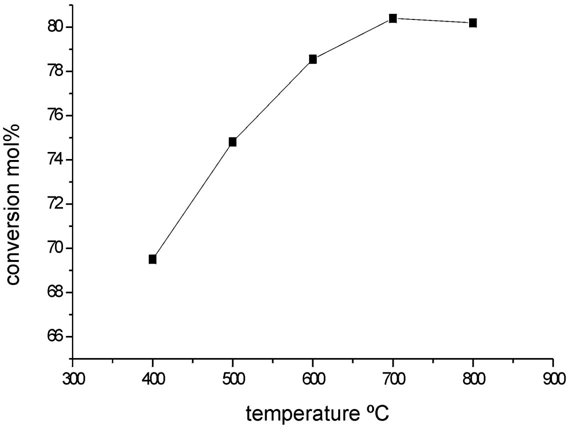

Fig. 2. Regeneration of HMAS-5 with Si/Al ratio of 61 at various temperatures.

3.6. TPD-NH$_3$ for HMAS-5, HMCM-41 and HZSM-5 samples

Fig. 3 shows curves of TPD-NH$_3$ for HMCM-41, HMCM-41, and HZSM-5 with similar Si/Al ratio. HMCM-41 (Fig. 3A) exhibits a broad peak, giving at 340°C. HMAS-5 (Fig. 3B) shows a peak at 420°C. HZSM-5 (Fig. 3C) shows two typical desorption peaks appearing at about 300 and 480°C, corresponding to its weak and strong acidic sites, respectively. These results indicate that the acidic strength of HMAS-5 is much stronger than that of HMCM-41, which could be responsible that HMAS-5 exhibits higher activity in the catalytic cracking.

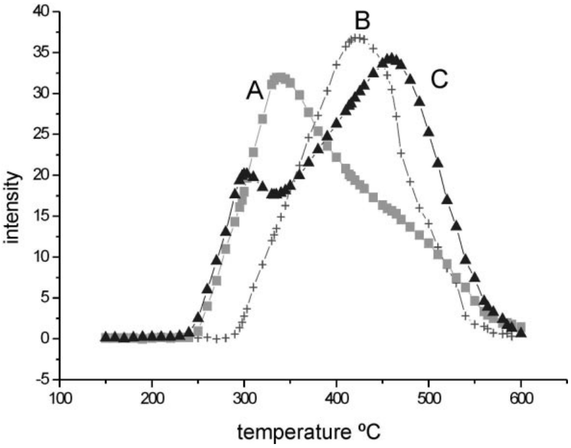

Fig. 3. TPD-NH$_3$ curves of (A) HMCM-41 (–■- -); (B) HMAS-5 (–+–); (C) HZSM-5 (–▲–). Si/Al ratio of HMCM-41, HMAS-5, and HZSM-5 is 60, 61, and 64, respectively.

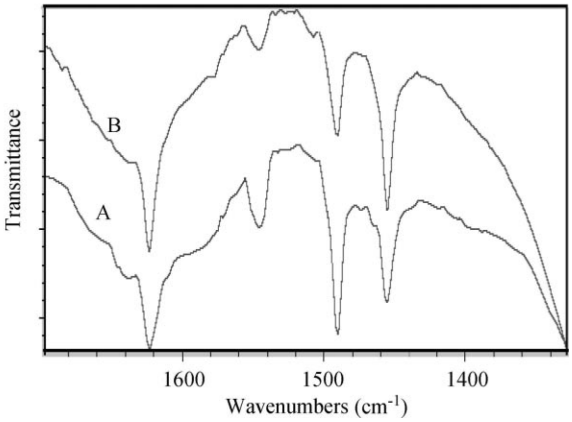

Fig. 4. IR spectra of pyridine adsorbed on (A) HMAS-5; (B) HMCM-41(Si/Al ratio of HMCM-41, HMAS-5 is 60 and 61, respectively).

3.7. IR spectra of pyridine adsorption over HMAS-5 and HMCM-41

IR spectra of pyridine adsorbed on HMAS-5 and HMCM-41 samples are shown in Fig. 4, giving the bands at 1450, 1490, and 1540 cm^{-1}, respectively. The band at 1450 cm^{-1} is assigned to Lewis acidic sites, and the band at 1540 cm^{-1} is assigned to Bronsted acidic sites on the samples [19–22].

It is interesting to note that at the same temperature HMAS-5 exhibits much higher concentration of Bronsted sites than those of HMCM-41, although their Lewis sites are similar. These results suggest that the contribution of Bronsted sites is larger than that of Lewis sites in the catalytic cracking, which is well consistent with those reported before [23–25].

4. Conclusions

A stable mesoporous aluminosilicate with hexagonal symmetry (MAS-5) has been synthesized by the co-templates of TEAOH and CTAB cationic surfactant. Catalytic data in the cracking of 1,3,5-triisopropylbenzene show that the conversion over HMAS-5 is higher than that over HA1MCM-41, which is assigned to the fact that HMAS-5 has stronger acidity than HA1MCM-41. These results have been demonstrated by temperature-programmed desorption of ammonia and infrared spectra of pyridine adsorbed on HMAS-5 and HMCM-41. Furthermore, we observed that the catalytic conversion over HMAS-5 is much higher than that over HZSM-5, which is assigned to the fact that the smaller pores of HZSM-5 is inaccessible to the larger molecule of 1,3,5-triisopropylbenzene.

Acknowledgements

This work was supported by the Foundation of the State Education Commission of China, the National Natural Science Foundation of China (grant number of 29825108 and 29733070), the National Advanced Materials Committee of China (NAMCC), and the Foundation of Key Laboratory for Inorganic Synthesis and Preparative Chemistry.

References

[1] M.E. Davis, Chem. Ind. 4 (1992) 137.
[2] M. Estermann, L.B. McCusker, C. Baerlocher, A. Merroche, H. Kessler, Nature 352 (1991) 320.
[3] C.T. Kresge, M.E. Leonowicz, W.J. Rochh, J.C. Vartuli, J.S. Beck, Nature 359 (1992) 710.
[4] J.S. Beck, J.C. Vartuli, W.J. Roch, M.E. Leonowicz, C.T. Kresge, K.D. Schmitt, C.T.W. Chu, D.H. Olson, E.W. Sheppard, S.B. McCullen, J.B. Higgins, J.C. Schlenker, J. Am. Chem. Soc. 114 (1992) 10834.
[5] W.O. Haag, R.M. Lago, P.B. Weisz, Disc. Faraday Soc. 72 (1981) 317.
[6] D.H. Olson, W.O. Haag, in: T.E. Whytes (Ed.), Catalytic Materials, ACS Symposium Series, Vol. 248, American Chemical Society, Washington, DC, 1984, p. 257.
[7] A. Corma, Chem. Rev. 97 (1997) 2373–2419.
[8] D. Zhao, J. Feng, Q. Huo, N. Melosh, G.H. Fredrichson, B.F. Chmelka, G.D. Stucky, Science 279 (1998) 23.
[9] S.S. Kim, Z. Zhang, T.J. Pinnavaia, Science 282 (1998) 1302.
[10] J.E. Naber, K.P. de Jong, W.H.J. Stock, H.P.C.E. Kuipers, M.F. Post, Stud. Surf. Sci. Catal. 84 (1994) 2197.
[11] W.F. Hoelderich, M. Hesse, F. Naumann, Angew. Chem. Int. Ed. Eng. 27 (1998) 226.
[12] W.O. Haag, Stud. Surf. Sci. Catal. 84 (1994) 1375.
[13] W.A. Wachter, US Patent 5 221 648 (1993).
[14] D.W. Breck, Zeolite Molecular Sieves, Wiley, New York, 1974.
[15] Z. Zhang, S. Qiu, F.-S. Xiao, et al., Unpublished result.
[16] H. Koch, W. Reschetilowski, Micropor. Mesopor. Mat. 25 (1998) 127–129.
[17] T. Ono, H. Kudo, M. Anpo, Appl. Catal. 194–195 (2000) 71.
[18] R.A. Pachovsky, B.W. Wojciechowski, Can. J. Chem. Eng. 49 (1971) 365.

[19] J.W. Ward, Infrared studies of zeolite surfaces and surface reactions, in: J. Rabo (Ed.), Zeolite Chemistry and Catalysis, American Chemical Society, Washington, DC, 1976.

[20] L.H. Little, Infrared Spectra of Adsorbed Species, Academic Press, New York, FL, 1966.

[21] M.L. Hair, Infrared Spectra in Surface Chemistry, Marcel Dekker, New York, 1967.

[22] K. Tanabe, H. Hattor, Y. Yanaguchi, T. Tanaka, Acid–Base Catalysis, Kadansha, Tokyo, 1988, p. 491.

[23] A. Aucejo, M.C. Burguet, A. Corma, V. Fornes, Appl. Catal. 22 (1986) 187.

[24] A. Corma, H. Garcia, J. Primo, Zeolites 11 (1991) 593.

[25] M. Trombetta, G. Bisca, M. Lenarda, L. Storaro, R. Ganzerla, L. Piovesan, A.J. Lopez, M.A. Rodriguez, E.R. Castellon, Appl. Catal. 193 (2000) 55.